Modeling of gas flow in cutting kerf using computational fluid dynamics

Upendra Tuladhar[1], Sang-Hyun Ahn[2, 3], Dae-Won Cho[2, *], Seokyoung Ahn[1], Tae Hyung Na[4]

[1]*School of Mechanical Engineering, Pusan National University, Busan, Republic of Korea*
[2]*Busan Machinery Research Center, Korean Institute of Machinery and Materials, Busan, Republic of Korea*
[3]*Department of Mechanical Engineering, Pukyong National University, Busan, Republic of Korea*
[4]*Decommissioning Technology Group, CRI, KHNP Co., Ltd, Daejeon, Republic of Korea*

**Corresponding Author: dwcho@kimm.re.kr*

1. Introduction

Thermal cutting is one of the most important production processes, and is widely employed in industrial processes like welding, assembling and riveting. Thermal cutting primarily means the use of energy in various forms to cut virtually any shape from iron and nonferrous materials out of sheets or large slabs. During the thermal cutting process, a high pressure gas is injected through nozzle along with the heat source to assist the cutting process by providing a mechanical force which ejects the melt and protects the nozzle from spatter [1].

During the cutting process, the high pressure assisting gas exiting the nozzle is usually associated with the occurrence of a non-desirable aerodynamics phenomena such as the presence of shock structures (i.e., Mach disks) resulting in the deterioration of the dynamic characteristics of the exit jet [2]. Several studies have investigated the gas flow dynamics in the gas-assisted thermal cutting process. The research works consist of both numerical simulations and experimental observations of gas flow characteristics. The authors in [3–6] investigated the interaction of gas flows within the cut kerf in order to study the dynamic characteristics of the exit jet at various stand-off distances during the laser cutting process. Cho et al. [7] captured the gas flow as a function of the inlet pressure and the stand-off distance using a high-speed camera with the Schlieren method. They used images before and after the gas injection to obtain the image intensity, which was applied to analyze the cutting gas flow for three different parts. They reported that the stronger the inlet pressure and the shorter the stand-off distance, the higher the image intensity value, and the higher the gas flow rate, respectively. Darwish et al. investigated the effect of inlet stagnation pressure and nozzle geometry on the behavior of the gas flow [8]. They modeled the jet flow through these nozzles numerically and verified them experimentally, using Schlieren visualization.

Most of the researches discussed above are carried out in carried out free flow. However, the gas flow behavior inside the cut kerf channel is different from the free flow. Therefore, the aim of the present study was to investigate the gas flow behavior inside the cut kerf and develop a numerical modeling using CFD.

2. Numerical modelling

The compressible and turbulent flow flowing through the nozzle into the cut kerf is assumed to be three dimensional, steady-state and employs standard *k-ω* turbulent model. For pressure-velocity coupling, a coupled algorithm is employed.

7.1. Governing equations

Based on the above assumptions, the governing equations to be solved in this numerical simulation include mass, momentum, and energy equations and are given as follow:

$$\frac{\partial \rho}{\partial t} + \nabla \cdot (\rho \mathbf{u}) = 0 \tag{1}$$

$$\rho\left(\frac{\partial \mathbf{u}}{\partial t} + \mathbf{u} \cdot \nabla \mathbf{u}\right) = -\nabla p + \nabla \cdot [\mu(\nabla \mathbf{u} + (\nabla \mathbf{u})^T)] + \nabla \cdot [\lambda(\nabla \cdot \mathbf{u})\mathbf{I}] \tag{2}$$

$$\frac{\partial}{\partial t}\rho\left(e + \frac{1}{2}u^2\right) + \nabla \cdot \left[\rho \mathbf{u}\left(e + \frac{1}{2}u^2\right)\right] = \nabla \cdot (\kappa \nabla T) + \nabla \cdot [-p\mathbf{u} + \boldsymbol{\tau} \cdot \mathbf{u}] \tag{3}$$

where, ρ is density, $\mathbf{u}$ and u represents velocity, p is pressure, μ and λ are dynamic and bulk viscosities respectively, $\mathbf{I}$ is an Identity tensor, e is internal (thermal) energy, κ is thermal conductivity, T is temperature, $\boldsymbol{\tau}$ is viscous stress tensor and the subscript T is matrix transformation.

To complete the model, a suitable expression is required for turbulent kinematic viscosity μ_t. For *k-ω* turbulent model (whose detailed transport equation can be found in [9, 10], and is omitted here for brevity) the turbulent kinematic viscosity μ_t is calculated from turbulent kinetic energy (k) and specific turbulence dissipation (ω) as in Equation 4.

$$\mu_t = \alpha^* \frac{\rho k}{\omega} \tag{4}$$

where, the coefficient α^* is given by Equation 5.

$$\alpha^* = \alpha_\infty^* \left(\frac{\alpha_0^* + Re_t/R_k}{1 + Re_t/R_k} \right) \quad (5)$$

where, α_∞^*=1, $Re_t = \rho k/\mu\omega$, R_k=6 and α_0^*=0.024.

7.2. Mesh generation and boundary condition

The CAD model was prepared using Solidworks 2017 then the numerical domain was modeled in design modeler of ANSYS workbench and finally tetrahedral mesh was generated in the numerical domain as shown in Figure 1(a-c). The total number of cells present in the mesh model was 1,596,084.

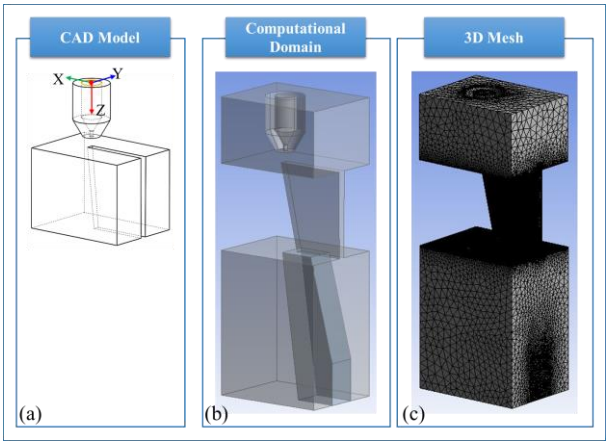

Fig. 1. CFD model (a) 3D CAD model, (b) Computational domain, (c) 3D Mesh

3. Results and discussion

The velocity and pressure fields along the symmetry plane of the computational domain were mapped to evaluate their validity with respect to the experimental results. Figure 1 shows the velocity map and the velocity distribution curve along the line passing through the cut kerf. Figure 2 shows the pressure map and the velocity distribution curve along the line passing through the cut kerf.

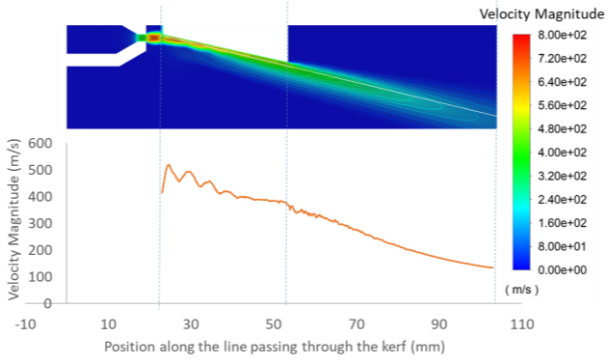

Fig. 2. Velocity field map and distribution curve along kerf slot.

The flow distribution along the nozzle and kerf slot for the tested turbulent model shows uniformity and have good flow distribution. The pressure distribution along the flow direction shows fluctuations, and follows a harmonic wave pattern, and dampens as the flow propagates further away. This is common for high pressure flow. And each oscillation represents Mach shock disc as reported by other researchers. The results were validated with the images obtained from Schlieren experiments.

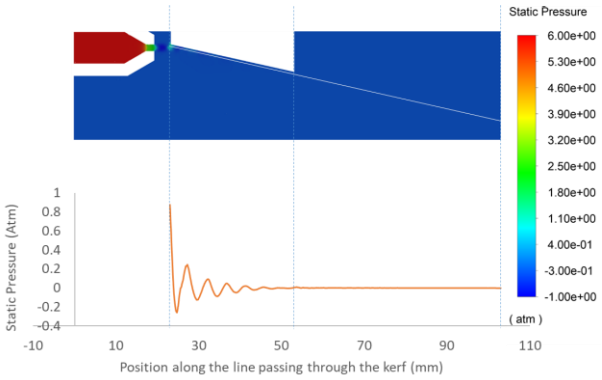

Fig. 2. Pressure field map and distribution curve along kerf slot.

4. Conclusions

The gas flow behavior inside the cutting kerf slot affects the cutting quality and the performance of the gas-assisted thermal cutting process to a great extent. Therefore studying the dynamic behavior of the flow inside the kerf can help operators effectively determine the optimum operating conditions. In this study, numerical modelling was carried out to investigate the gas flow dynamics inside the kerf slot. The turbulent model employed in this study showed consistency with other studies and could be validated with Schlieren experiment results.

Acknowledgements

This work was supported by the Korea Institute of Energy Technology Evaluation and Planning (KETEP) granted financial resource from the Ministry of Trade, Industry & Energy, Republic of Korea (No. 20201520300060), National Research Foundation of Korea (NRF) grant funded by the Korean government (MSIP: Ministry of Science, ICT and Future Planning) (No.2017M2B2B1072888) and the Korea Institute of Machinery and materials (NK238A, NK238C).

REFERENCES

[1] M. Darwish, L. Orazi, and D. Angeli, Simulation and Analysis of the Jet Flow Patterns from Supersonic Nozzles of Laser Cutting Using Openfoam, The Int. J. of Advanced Manufacturing Technology, Vol. 102, No. 9, pp. 3229–3242, 2019.
[2] I.S. Chang, and W.L. Chow, Mach Disk from Underexpanded Axisymmetric Nozzle Flow, AIAA Journal, Vol. 12, No. 8, pp. 1079–1082, 1974.
[3] J. Hu, Z. Zhang, J. Luo, and X. Sheng, Simulation and Experiment on Standoff Distance Affecting Gas Flow in Laser Cutting, Applied Mathematical Modelling. Vol. 35, No. 2, pp. 895–902, 2011.
[4] C. Mai, and J. Lin, Flow Structures Around an Inclined Substrate Subjected to A Supersonic Impinging Jet in Laser Cutting, Optics and Laser Technology, Vol. 34, No. 6, pp. 479–486, 2002.
[5] K. Chen, Y. Yao, and V. Modi, Gas Dynamic Effects on Laser Cut Quality, Journal of Manufacturing Processes. Vol. 3, pp. 38–49, 2001.
[6] H. Jun, S.J. Guo, L. Lei, and Z. Yao, Characteristic Analysis of Supersonic Impinging Jet in Laser Machining, The International Journal of Advanced Manufacturing Technology, Vol. 39, pp. 716–724, 2008.
[7] D.-W. Cho, J. Choi, S. Lee, and D. Shin, Analysis of Gas Flow Behavior in the Laser Cutting Process using the Schlieren Method and Image Processing, Journal of Welding and Joining, Vol. 38, No. 6, pp. 569–575, 2020.
[8] M. Darwish, L. Mrňa, L. Orazi, and B. Reggiani, Numerical Modeling and Schlieren Visualization of the Gas-Assisted Laser Cutting Under Various Operating Stagnation Pressures, International Journal of Heat and Mass Transfer, Vol. 147, No. 118965, 2020.
[9] D.C. Wilcox, Turbulence Modeling for CFD, DCW Industries, La Canada, 1998.
[10] D.C. Wilcox, Formulation of the *k*-ω Turbulence Model Revisited, AIAA Journal, Vol. 46, No. 11, pp. 2823–2838, 2008.